

The Gestalt Computational Model

Yu Chen¹, Hongwei Lin^{1,*}, and Jiacong Yan¹

¹School of Mathematics Science, Zhejiang University, No. 866, Yuhangtang Road, Hangzhou, China
*hwlin@zju.edu.cn

ABSTRACT

Widely employed in cognitive psychology, Gestalt theory elucidates basic principles in visual perception, but meanwhile presents significant challenges for computation. The advancement of artificial intelligence requires the emulation of human cognitive behavior, for which Gestalt theory serves as a fundamental framework describing human visual cognitive behavior. In this paper, we utilize persistent homology, a mathematical tool in computational topology, to develop a computational model for Gestalt theory, addressing the challenges of quantification and computation. The Gestalt computational model not only holds promise for applications in artificial intelligence and computer vision, but also opens a new research direction of computational visual perception.

Introduction

The development of artificial intelligence now urgently requires computational models for visual perception¹. The Gestalt theory, formulated by psychologists Wolfgang Köhler, Kurt Koffka, and Max Wertheimer in the early 20th century and has been developed to this day, provides a classic framework for understanding visual perception²⁻⁴. Especially, Gestalt theory demonstrates the extraction of global properties in visual perception through experiments⁵⁻¹⁰. In this paper, we utilize persistent homology to calculate visual perceptual results that conform to Gestalt theory. On the one hand, this validates the extraction of global properties in the visual perception system by computation, rather than relying solely on experiments. On the other hand, the computational ability to derive visual perceptual results holds significant potential for applications in the fields of artificial intelligence and computer vision.

Emphasizing on organizing sensory information into coherent patterns and wholes, Gestalt theory asserts that each component of any visual perceptual outcome is interrelated, and the entirety is shaped by these connections. In essence, Gestalt theory explores the relationship between the whole and its parts, with the fundamental premise that the visual object is initially perceived as a unified whole and subsequently as parts. Moreover, the visual topology theory⁵ is developed to elucidate the global properties of Gestalt theory in terms of topological concepts. Visual topology theory interprets the concept of whole in Gestalt theory as large-scale topological features intrinsic to the perceived object, and then explores the relationship between the global and the local aspects in Gestalt theory from the perspective of algebraic topology⁷.

The Gestalt theory plays an important role in computer vision and artificial intelligence, which can help achieve more accurate and reasonable visual perceptual results. When applying Gestalt principles to the field of computer vision, it is crucial to develop a computational model for quantifying these principles and efficiently calculating the visual perceptual results. Several attempts have been made to quantify Gestalt theory¹¹. Hawkins et al.¹² proposed capacity coefficients to quantify the gap between the whole and the sum of its parts. Wei et al.¹³ introduced a method using the tilt aftereffect from visual adaptation to quantify grouping effects. However, these methods for quantifying Gestalt theory are based on experience or experiments to verify their effectiveness. Moreover, Bayesian hierarchical grouping is also a common method that treats Gestalt organization as a statistical inference problem¹⁴, but shows the limitations of relying on probabilistic priors and may lead to complex computation. Chen et al.^{5,7} quantified the Gestalt theory using the homology theory within tolerance space to interpret Gestalt theory from the perspective of visual topology theory, but no computational method is given. Peng et al.¹⁵ also employed tolerance space to compute the proximity and similarity principle for dot-pattern grouping. But this approach only addresses these two principles and is not generalized to some other key Gestalt principles such as closure and pragnanz. Therefore, the development of computational model for Gestalt theory still poses significant challenges.

Persistent homology, a novel computational tool that makes the classical homology theory computable, currently serves as a method for identifying topological features within target shapes¹⁶⁻²¹. The great significance of persistent homology lies in making many abstract concepts in algebraic topology efficiently computable, thus establishing a new branch known as computational topology. Moreover, topological data analysis (TDA), a powerful new branch for data processing, has been developed based on methods including persistent homology²²⁻²⁵. It has been successfully applied in various fields such as biomedicine²⁶, oncology²⁷, chemical engineering²⁸, and machine learning²⁹⁻³⁴, etc.

Since visual topology theory utilizes classical algebraic topology to interpret Gestalt theory, and persistent homology makes algebraic topology concepts efficiently computable, persistent homology can be employed to calculate key Gestalt principles, e.g., similarity, proximity, closure, good continuation and pragnanz^{3,4,35}. In this paper, we will elaborate on the underlying mechanisms of these principles within the context of persistent homology, and develop the computational model for Gestalt theory. The computation results demonstrate that persistent homology is an efficient and straightforward tool for calculating Gestalt theory.

Results

Gestalt computational model

We now introduce the computational model for Gestalt theory, using persistent homology and the corresponding persistence diagram (PD) based on the Vietoris–Rips complex (VR complex) and Vietoris–Rips filtration (VR filtration)¹⁶. It should be noted that, in the VR filtration, a series of nested VR complex will be generated,

$$VR(\varepsilon_0) \subset VR(\varepsilon_1) \subset \cdots \subset VR(\varepsilon_i) \subset VR(\varepsilon_{i+1}) \subset \cdots \subset VR(\varepsilon_N),$$

where $\varepsilon_0 = 0 < \varepsilon_1 < \cdots < \varepsilon_i < \varepsilon_{i+1} < \cdots < \varepsilon_N$. Moreover, in the PDs presented in this paper, the red points represent points in the zero-dimensional persistence diagram, and the blue points represent points in the one-dimensional persistence diagram. The computational model for Gestalt theory is detailed as follows, where the perceived objects are represented as a planar point set

$$\{\mathbf{P}_i = (x_i, y_i), i = 1, 2, \cdots, n\}. \quad (1)$$

Here for an object that appears to have a size, such as a dot, (x_i, y_i) represents its barycenter coordinate.

1. *Extra coordinates assignment*: Assign each point extra z -coordinates according to the attributes influencing perception, that is, color, shape, size, to name a few. And the planar point set is changed to the point set in $(m + 2)$ -dimensional space, i.e.,

$$\{\mathbf{Q}_i = (x_i, y_i, z_{i,1}, z_{i,2}, \cdots, z_{i,m})\} \quad (2)$$

where $i = 1, 2, \cdots, n$. The extra z -coordinates are taken according to features, e.g., color, shape, size, etc.

2. *PD calculation*: Construct VR filtration based on the point set and compute the corresponding persistence diagrams. Typically, only the zero-dimensional persistence diagrams (0-PDs) or one-dimensional persistence diagrams (1-PDs) is employed in the Gestalt computational model.
3. *Point clustering*: Project the points in a PD onto the line $y = -x$, and cluster the projected points into two classes using, for example, k -means algorithm³⁶ ($k = 2$). While the class closer to the origin $(0, 0)$ corresponds to the noise points, called noise class; the class farther away to the origin corresponds to the significant points with greater persistence, called significant class.
4. *Threshold determination*: Determine a suitable threshold ε_g . For 0-PD, ε_g should be greater than the largest death time t_d of the noise points, and less than the smallest death time of the significant points; for 1-PD, ε_g should be greater than the largest birth time t_b of the significant points, and less than the smallest death time of the significant points. At the VR complex with the parameter ε_g , i.e., $VR(\varepsilon_g)$, all significant topological features, such as significant connected components or loops, exist. By default, we set $\varepsilon = t_d$ (for 0-PD) or $\varepsilon = t_b$ (for 1-PD).
5. *Perception result reconstruction*: Reconstruct the visual perceptual results from the VR complex with the parameter ε_g , i.e., $VR(\varepsilon_g)$. The reconstructed visual perceptual results satisfy the Gestalt principles.

Similarity principle

To demonstrate the Gestalt computational model, we employ it to calculate the visual perceptual results dominated by the Gestalt similarity principle. According to the similarity principle, when objects are relatively similar in shape, size, color or other attributes, these objects appear to be grouped together. In the following instance of calculating the similarity principle via the Gestalt computational model developed above, only one extra coordinate $z_{i,1}$ for color is required (see Fig. 1 a and d). We set $z_{i,1} = 10$ for blue points and $z_{i,1} = 0$ for red points. When calculating the subsequent Gestalt principles, $z_{i,1}$ is also set up in the same manner. First we take the point set in Fig. 1 a as an example. After the extra coordinate for color is assigned, the VR filtration is constructed, and the 0-PD is generated (refer to Fig. 1 b). And the construction of VR filtration is depicted in Supplementary Video 1 in the Supplementary Information). Next, the points in the 0-PD are projected onto the line $y = -x$, and

they are clustered into two classes with 2-means clustering method. The significant class contains seven significant points with coordinates $(0, +\infty)$, $(0, 11.18033981)$, and $(0, 10)$ (occurring five times), and the noise class includes three points, each with coordinate $(0, 5)$. Consequently, we take the threshold $\varepsilon_g = 5$, and the VR complex $VR(5)$ (Fig. 1 c) is the visual perceptual result, which satisfies the Gestalt similarity principle very well. That is, the points with the same color are grouped together.

In Fig. 1 d, there is another example for similarity principle, i.e., a grid of red dots. After constructing the VR filtration, generating the 0-PD, and clustering the points in the 0-PD (Fig. 1 e), the threshold ε_g can be set as $\varepsilon_g = 5$. The VR complex $VR(5)$ is demonstrated in Fig. 1 f, which is the calculation result by the Gestalt computational model. The result in Fig. 1 f forms a lattice, satisfying the Gestalt theory perfectly.

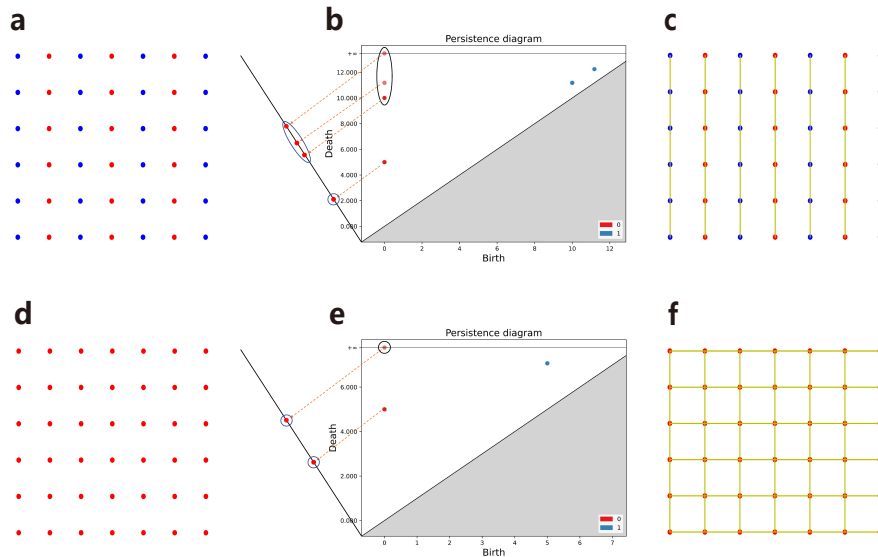


Figure 1. Calculation of Gestalt similarity principle. a, d, Examples for similarity principle. b, e, The clustering result of the corresponding 0-PD with highlighted zero-dimensional significant points. c, f, The VR complex $VR(\varepsilon_g)$ that coincides with the similarity principle.

In the following, we will briefly introduce the calculation of other Gestalt principles, including proximity, closure, good continuation and pragnanz, using the Gestalt computational model. Details of the calculation are provided in the Supplementary Information, as well as the videos of the VR filtration procedure.

Proximity principle

The Gestalt proximity principle states that objects close or neighboring in space appear to be grouped together. The point set exemplifying the proximity principle is illustrated in Fig. 2 a. After clustering the points in the 0-PD (Fig. 2 b), it is found that there are four points in the significant class, corresponding to four connected components in the corresponding VR complex. The computational result is the VR complex demonstrated in Fig. 2 c, which conforms to the Gestalt proximity principle, i.e., the dots are perceived as four columns.

Closure principle

The Gestalt closure principle claims that though some shapes are not closed, our minds have a tendency to complete them, filling in the gaps to perceive them as a whole. Take the point set in Fig. 2 d as an example. According to the Gestalt computational model, there is only one significant point in the 1-PD (Fig. 2 e), representing the hidden one-dimensional topological feature (i.e., loop) within the original point set (Fig. 2 d). The VR complex with the significant topological feature, i.e., the computational result derived from Gestalt computational model, is illustrated in Fig. 2 f, where the shape hidden in the original point set in Fig. 2 d is correctly closed.

Good continuation principle

The Gestalt good continuation principle states that points that form straight lines or smooth curves when connected are perceived as belonging together, and these lines or curves tend to be seen as connected in the smoothest way possible. Now, we employ the Gestalt computational model to process the point set in Fig. 2 g. After clustering the points in the 1-PD (Fig. 2 h), we get the threshold $\varepsilon_g = 1.2815$. The last step for the computation of good continuation, i.e., reconstructing the visual perceptual results,

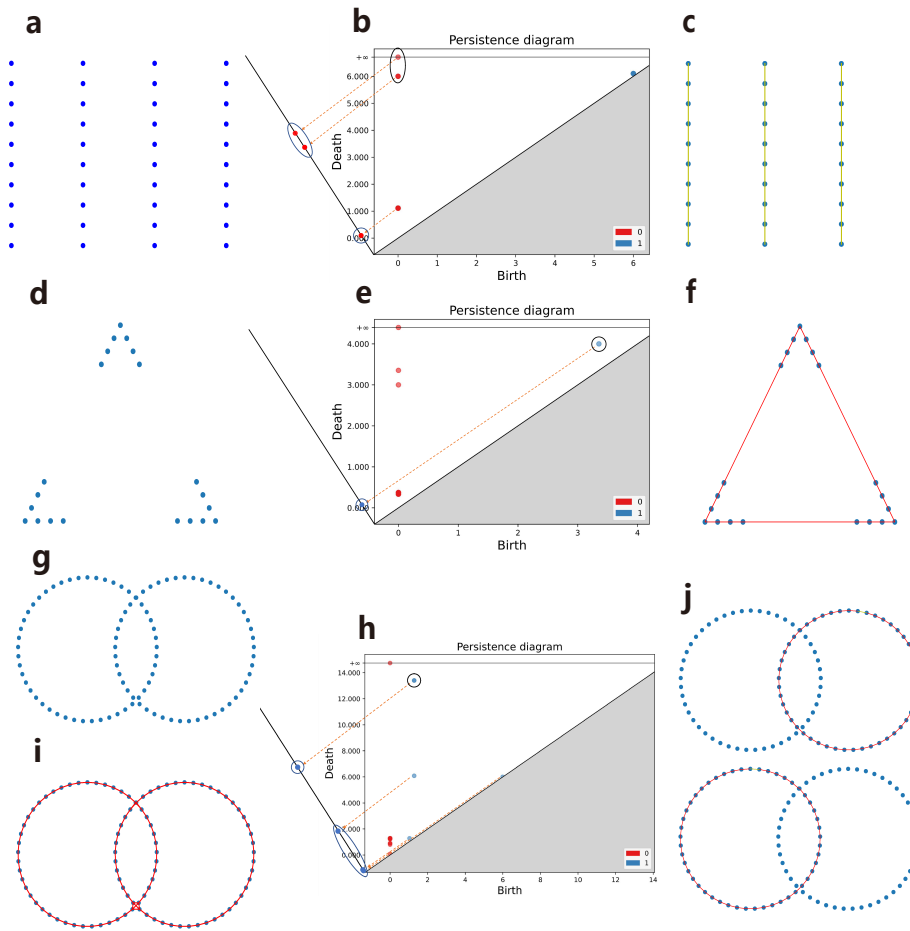


Figure 2. Calculation of the principle of proximity, closure and good continuation. a, d, g, Examples of Gestalt proximity, closure and good continuation principles. b, The clustering result of the corresponding 0-PD with highlighted zero-dimensional significant points. c, The VR complex $VR(\mathcal{E}_g)$ that coincides with the Gestalt proximity principle. e, h, The clustering result of the corresponding 1-PD with highlighted one-dimensional significant points. f, The hidden loop in the point cloud. i, The corresponding 1-skeleton when all one-dimensional topological features (loops) have formed. j, Two circles are successfully identified. Here edges whose two terminal nodes are the starting and ending points are drawn in yellow.

is more complicated, comparing with the Gestalt principles above. First, we extract the 1-skeleton (which is composed of only 0-simplex and 1-simplex)¹⁶ of the VR complex $VR(1.2815)$ (Fig. 2 i). This 1-skeleton serves as a good approximation of the shape represented by the original point set. Then, we select a starting point and an ending point in the 1-skeleton, corresponding to the two terminal nodes of an edge in the 1-skeleton in this example (Fig. 2 i). Beginning from the starting point, we search for the next point along the direction with the smallest steering angle, continuing until the ending point is reached, thereby forming a branch of the shape (Fig. 2 j). In this way, each branch of the shape can be traced out (Fig. 2 j). The shapes in Fig. 2 j calculated by the Gestalt computational model conform to the good continuation principle well.

Pragnanz principle

The Gestalt pragnanz principle, also known as simplicity principle, asserts that every stimulus will be perceived in the simplest possible manner. Specifically, during the process of perception, individuals tend to comprehend these global topological features in a straightforward manner, focusing on significant topological features and providing a simple understanding, while disregarding unimportant features. For instance, one tends to perceive the shape of the five Olympic rings as the five circles (Fig. 3 a) rather than the nine sections (Fig. 3 b)³⁵. By the Gestalt computational model, considering the point cloud in Fig. 3 c that represents the shape of the five Olympic rings, we cluster the points in the 1-PD (Fig. 3 d), and then get five significant points in the significant class, corresponding to five significant features (the five circles, see Fig. 3 e). The VR complex $VR(\mathcal{E}_g)$ (Fig. 3 e) is the computational result, which keeps the significant topological features, and discards the unimportant features, thus satisfying the pragnanz principle.

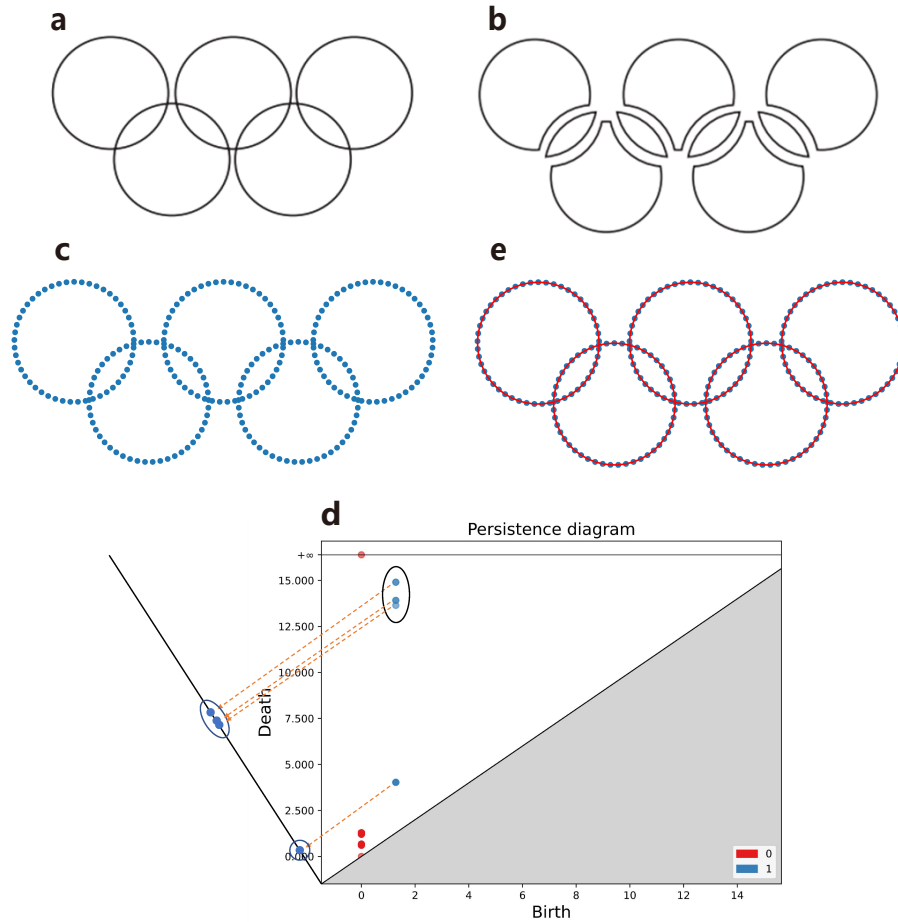


Figure 3. Calculation of Gestalt pragnanz principle. a, The shape of the five Olympic rings. b, It is unlikely that the shapes in Fig. 3 a will be seen as nine parts. c, An example of the pragnanz principle. The point cloud represents the shape of the five Olympic rings. d, The clustering result of the corresponding 1-PD with highlighted one-dimensional significant points. e, Five circles that represent five significant topological features correspond to the five significant points in the 1-PD.

Conflicts between different principles

Lastly, we will deal with the conflicts between different Gestalt principles using the developed Gestalt computational model. In practice, conflicts between Gestalt principles, such as the conflict between the proximity principle and the similarity principle, as well as conflicts within the similarity principle itself due to different attributes, are common occurrences. This presents an important research issue. Using persistent homology, our model provides a quantitative method to explore these conflicts by selectively controlling a dominant principle or attribute. An example of a conflict between different attributes of the similarity principle itself is depicted in Fig. 4. In the illustrated grid of points (Fig. 4 a), each row shares the same shape, and each column shares the same color, with two additional z -coordinate values added to each point, i.e., $z_{i,1}$ for color and $z_{i,2}$ for shape. Consequently, each planar point corresponds to a 4-dimensional coordinate, where each point in the point set (1) is located at the barycenter of each shape. By adjusting the salience of these attributes, we can control which of the two will be the dominant attribute. For example, if we assign a greater difference value to the shape than to the color, then upon computing and clustering the 0-PD and selecting parameter ε_g , we obtain the VR complex $VR(\varepsilon_g)$. This VR complex illustrates that the points will be classified according to the shape attribute (Fig. 4 c). Conversely, if we assign a greater difference value to the color than to the shape, again by computing and clustering the 0-PD and selecting $VR(\varepsilon_g)$, we can see that the points will be classified according to the color attribute (Fig. 4 d). This suggests that the Gestalt computational model, rooted in persistent homology, can effectively function as a versatile quantitative tool for investigating conflicts between Gestalt principles.

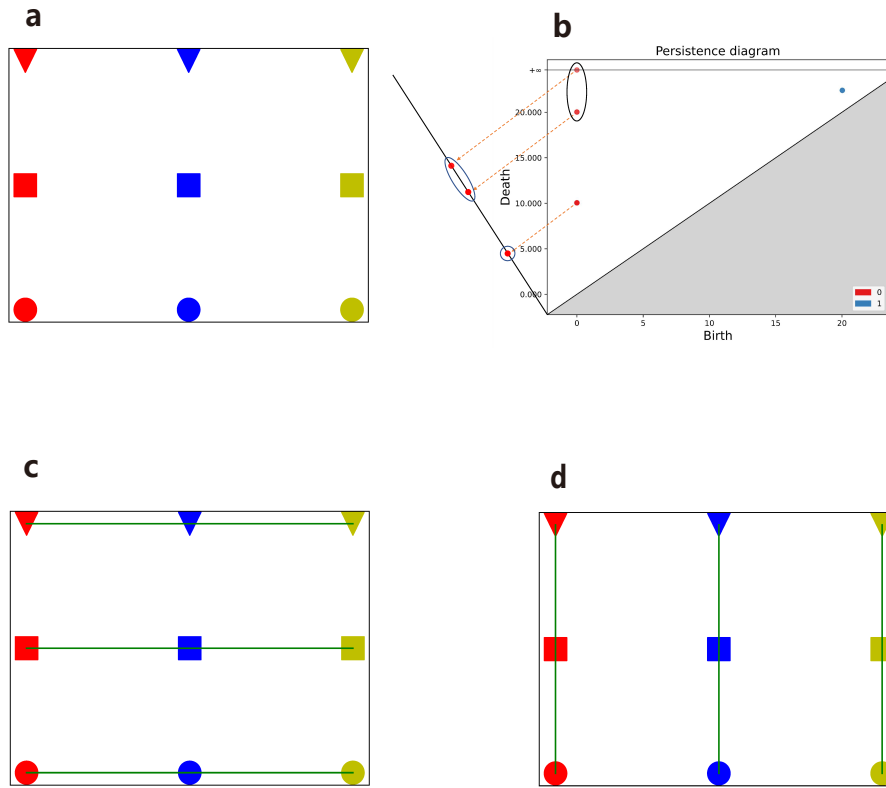


Figure 4. Illustration of conflicts. a, An example of a conflict between different attributes of the similarity principle itself. b, The clustering result of the corresponding 0-PD with highlighted zero-dimensional significant points. Here two situations lead to the same 0-PD. c, The computation result when the shape feature is dominant. d, The computation result when the color feature is dominant.

Discussion

We have developed a computational model for Gestalt theory using persistent homology, which integrates Gestalt theory from cognitive psychology with persistent homology in computational topology for the first time. This provides a clear description of the relationship between the global and local aspects in Gestalt theory. Additionally, the capacity of persistent homology to extract global topological features makes it a valuable tool for calculating Gestalt theory. Furthermore, our model has the capacity to combine Gestalt theory with computer vision and artificial intelligence, serving as the computational foundation for visual perception implemented in artificial intelligence.

Methods

Vietoris–Rips complex

The n -simplex is defined as the convex hull formed by $n + 1$ affine independent points $\{u_0, u_1, \dots, u_n\}$ in Euclidean space \mathbb{R}^N , denoted as $[u_0, u_1, \dots, u_n]$. An n -simplex can be represented by various geometric models, such as a vertex (0-simplex), a line segment (1-simplex), a triangle (2-simplex), and a tetrahedron (3-simplex). A (abstract) simplicial complex K is a collection of simplices that satisfies the following properties: every face of a simplex in K is also in K , and the intersection of any two simplices in K is a face of both of them³⁷. Moreover, we define the dimension of a simplicial complex K as the maximum dimension among all the simplices in K .

The Vietoris–Rips (VR) Complex¹⁶ is a type of simplicial complex. Its construction is defined by the following rules: for any $\varepsilon > 0$, a finite subset $\{x_0, x_1, \dots, x_n\} \subseteq X$ of the space \mathbb{R}^N forms a simplex $[x_0, x_1, \dots, x_n]$ if and only if the distance between

any pair of points x_i and x_j satisfies $d(x_i, x_j) \leq \varepsilon$. The collection of all simplices generated by the point cloud X that satisfy the aforementioned conditions constitutes the VR complex. It is worth noting that alternative definitions may employ a bound of 2ε instead of ε (i.e. $d(x_i, x_j) \leq 2\varepsilon$), resulting in the same combinatorial object but with filtration parameters that are half. Although this choice affects the filtration parameters, it does not alter the underlying combinatorial structure of the complex. Consequently, the extraction results of topological features are not affected.

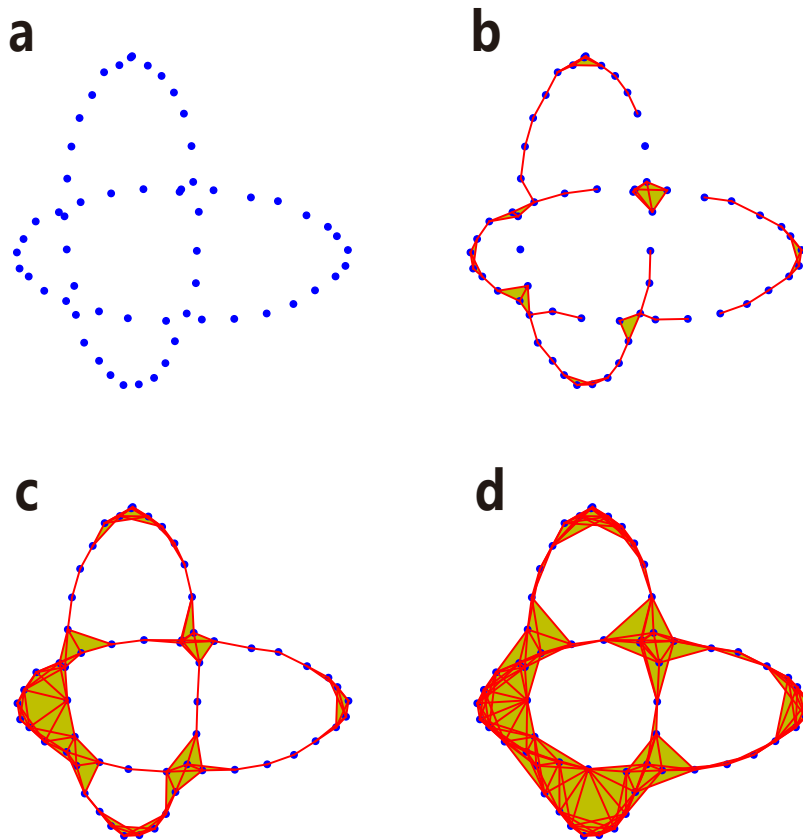


Figure 5. An example of VR filtration with parameter ε . a, b, c, d corresponds to $\varepsilon = 0.0, 1.0, 1.5, 2.0$ respectively. Here only simplices with dimension less than and equal to two are depicted.

Persistent homology

Let K be a simplicial complex and n its dimension. An n -chain is a sum of n -simplices in K , denoted by $c = \sum a_i \sigma_i$, where σ_i represents an n -simplex, and a_i is its coefficient belonging to an Abelian group, typically \mathbb{Z} or \mathbb{Z}_2 (in our work we use \mathbb{Z}_2 coefficients). With the addition operation, the n -chains form the n -chain group, denoted by $C_n(K)$.

The boundary for a n -simplex $\sigma = [x_0, x_1, \dots, x_n]$ is given by

$$\partial_n \sigma = \sum_{j=0}^n (-1)^j [x_0, \dots, \hat{x}_j, \dots, x_n],$$

where \hat{x}_j denotes the omission of x_j . Let $Z_n(K) = \text{Ker}(\partial_n)$ and $B_n(K) = \text{Im}(\partial_{n+1})$. The n -th homology group of K is defined as the quotient group $H_n(K) = Z_n(K)/B_n(K)$.

Persistent homology offers a multi-scale description of homology using filtration. Given a point cloud X and a series of parameters $0 = \varepsilon_0 < \varepsilon_1 < \dots < \varepsilon_m$, the nested VR complex sequence

$$VR(X, \varepsilon_0) \subset VR(X, \varepsilon_1) \subset \dots \subset VR(X, \varepsilon_m)$$

is referred to as a VR filtration¹⁶. Without confusing notation, we will also write $VR(X, \varepsilon)$ simply as $VR(\varepsilon)$. Fig. 5 shows an example of a VR filtration. If we regard each ε as one moment, then at each moment in the filtration there is a different VR complex, which is called the state corresponding to ε in the filtration.

If we denote each $VR(X, \varepsilon_i)$ as K_i ($0 \leq i \leq m$), then for every $i \leq j$ we have an inclusion map from K_i to K_j and therefore an induced homomorphism $f_p^{i,j} : H_p(K_i) \rightarrow H_p(K_j)$ for each dimension p . The p -th persistent homology groups¹⁶ are defined as the images of the homomorphisms induced by inclusion:

$$H_p^{i,j} = \text{Im } f_p^{i,j}, \forall 0 \leq i \leq j \leq m.$$

The corresponding p -th persistent Betti numbers are the ranks of these groups: $\beta_p^{i,j} = \text{rank } H_p^{i,j}$.

The standard method for computing the persistent homology of a filtration is the reduced matrix method¹⁶, and there are corresponding tools for computing persistent homology within many software packages and libraries. As the parameter ε increases, we can observe the birth time and death time of topological features (i.e. the representations of generators of persistent homology groups, which are also called cycles) in different dimensions. One of the most common tools for visualizing persistent homology is the persistence diagram (PD)¹⁶, as shown in Fig. 6 a, which can be calculated using tools such as the GUDHI Python module³⁸. The set of points that records the birth time and death time of the n -cycles are denoted as the n -PD. Each point in an n -PD takes the form (b_i, d_i) , representing an n -cycle and capturing its birth time b_i and death time d_i . It is clear that all points in a PD are located above the diagonal $y = x$. And the value $|d_i - b_i|$ is denoted as the persistence of this cycle. Moreover, a point in a persistence diagram is termed a multi-point if at least one other point exists at its location.

Clustering of points in a persistence diagram

We can identify the significant topological features of the underlying space from the persistence diagrams. To achieve this, it is necessary to locate the points in the n -PD that represent n -dimensional significant topological features. An effective approach involves clustering the points in the n -PD and extracting the class that exhibits the greater persistence.

To complete the clustering, initially we project the points in the given n -PD onto the line $y = -x$, which is perpendicular to the diagonal $y = x$ in the PD. It becomes apparent that the distances from the projected points to the origin $(0, 0)$ can effectively represent the persistence of the relevant points in the PD. If a point has a death time of $+\infty$, we can either skip it and directly classify it as a significant point, or replace its $+\infty$ coordinate with a suitably large value that will not affect the clustering results during the clustering process. For example, we can replace it with a value that is appropriately larger than the second largest death time among the other points. Subsequently, the projected points on $y = -x$ can be classified into two classes using a clustering algorithm, such as the k -means algorithm ($k = 2$). Fig. 6 b illustrates the process of clustering a PD. The points within the class demonstrating greater persistence correspond to significant topological features, referred to as significant points, while points within the other class correspond to noise features, referred to as noise points. If the PD contains only one point with positive persistence, we consider this point to be significant, indicating the existence of only the significant class. In our method, we primarily focus on the significant points in the PDs to illustrate the topological understanding of visual perception. Therefore, we will highlight these significant points on the obtained PDs.

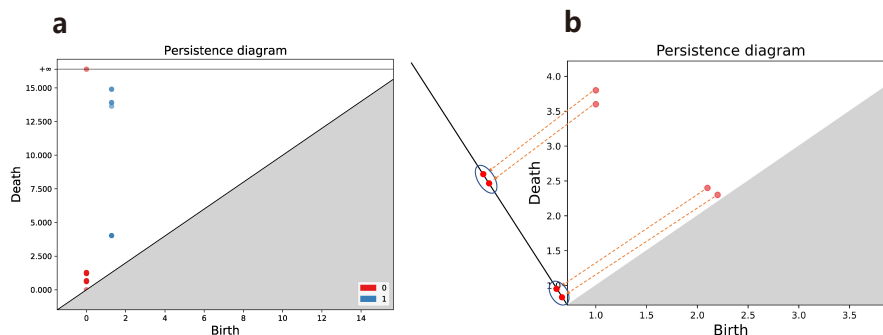


Figure 6. Illustration of persistence diagram. a, An example of persistence diagram. As the label shows, the red points in the persistence diagram represent the zero-dimensional persistence diagram, and the blue points represent the one-dimensional persistence diagram. b, The process of clustering points in the given n -PD based on persistence.

Data availability

The authors declare that the data supporting the findings of this study are available within the paper and supplementary information files.

References

1. Shiqiang Zhu, Ting Yu, Tao Xu, Hongyang Chen, Schahram Dustdar, Sylvain Gigan, Deniz Gunduz, Ekram Hossain, Yaochu Jin, Feng Lin, et al. Intelligent computing: the latest advances, challenges, and future. *Intelligent Computing*, 2:0006, 2023.
2. Wolfgang Köhler. Gestalt psychology. *Psychologische Forschung*, 31(1):XVIII–XXX, 1967.
3. Kurt Koffka. Principles of Gestalt psychology, volume 44. Routledge, 2013.
4. Max Wertheimer. Laws of organization in perceptual forms. *Psychologische Forschung*, 4, 1923.
5. Lin Chen. Topological structure in visual perception. *Science*, 218(4573):699–700, 1982.
6. Yan Zhuo, Tian Gang Zhou, Heng Yi Rao, Jiong Jiong Wang, Ming Meng, Ming Chen, Cheng Zhou, and Lin Chen. Contributions of the visual ventral pathway to long-range apparent motion. *Science*, 299(5605):417–420, 2003.
7. Lin Chen. The topological approach to perceptual organization. *Visual Cognition*, 12(4):553–637, 2005.
8. Shihui Han, Glyn W Humphreys, and Lin Chen. Uniform connectedness and classical gestalt principles of perceptual grouping. *Perception & psychophysics*, 61(4):661–674, 1999.
9. Lixia He, Jun Zhang, Tiangang Zhou, and Lin Chen. Connectedness affects dot numerosity judgment: Implications for configural processing. *Psychonomic bulletin & review*, 16(3):509–517, 2009.
10. Jeremy M Wolfe and Todd S Horowitz. What attributes guide the deployment of visual attention and how do they do it? *Nature reviews neuroscience*, 5(6):495–501, 2004.
11. Frank Jäkel, Manish Singh, Felix A Wichmann, and Michael H Herzog. An overview of quantitative approaches in gestalt perception. *Vision research*, 126:3–8, 2016.
12. Robert XD Hawkins, Joseph W Hout, Ami Eidels, and James T Townsend. Can two dots form a gestalt? measuring emergent features with the capacity coefficient. *Vision research*, 126:19–33, 2016.
13. Ning Wei, Tiangang Zhou, and Lin Chen. Objective measurement of gestalts: Quantifying grouping effect by tilt aftereffect. *Behavior research methods*, 50:963–971, 2018.
14. Vicky Froyen, Jacob Feldman, and Manish Singh. Bayesian hierarchical grouping: Perceptual grouping as mixture estimation. *Psychological Review*, 122(4):575, 2015.
15. Peng Peng, Kai-Fu Yang, and Yong-Jie Li. A computational model for gestalt proximity principle on dot patterns and beyond. *Journal of Vision*, 21(5):23–23, 2021.
16. Herbert Edelsbrunner and John L Harer. Computational topology: an introduction. American Mathematical Society, 2022.
17. Afra Zomorodian and Gunnar Carlsson. Computing persistent homology. In *Proceedings of the twentieth annual symposium on Computational geometry*, pages 347–356, 2004.
18. Edelsbrunner, Letscher, and Zomorodian. Topological persistence and simplification. *Discrete & Computational Geometry*, 28:511–533, 2002.
19. Herbert Edelsbrunner, John Harer, et al. Persistent homology—a survey. *Contemporary mathematics*, 453(26):257–282, 2008.
20. Peter Bubenik and Peter T Kim. A statistical approach to persistent homology. *Homology, homotopy and Applications*, 9(2):337–362, 2007.
21. David Cohen-Steiner, Herbert Edelsbrunner, and John Harer. Stability of persistence diagrams. In *Proceedings of the twenty-first annual symposium on Computational geometry*, pages 263–271, 2005.
22. Afra Zomorodian. Topological data analysis. *Advances in applied and computational topology*, 70:1–39, 2012.
23. Larry Wasserman. Topological data analysis. *Annual Review of Statistics and Its Application*, 5:501–532, 2018.
24. Elizabeth Munch. A user’s guide to topological data analysis. *Journal of Learning Analytics*, 4(2):47–61, 2017.
25. Frédéric Chazal and Bertrand Michel. An introduction to topological data analysis: fundamental and practical aspects for data scientists. *Frontiers in artificial intelligence*, 4:108, 2021.

26. Yara Skaf and Reinhard Laubenbacher. Topological data analysis in biomedicine: A review. *Journal of Biomedical Informatics*, 130:104082, 2022.
27. Anuraag Bukkuri, Noemi Andor, and Isabel K Darcy. Applications of topological data analysis in oncology. *Frontiers in artificial intelligence*, 4:659037, 2021.
28. Alexander D Smith, Paweł Dłotko, and Victor M Zavala. Topological data analysis: concepts, computation, and applications in chemical engineering. *Computers & Chemical Engineering*, 146:107202, 2021.
29. Gunnar Carlsson, Rick Jardine, Dmitry Feichtner-Kozlov, Dmitriy Morozov, Frédéric Chazal, Vin de Silva, Brittany Fasy, Jesse Johnson, Matt Kahle, Gilad Lerman, et al. Topological data analysis and machine learning theory. In *Proc. BIRS Workshop*, pages 1–11, 2012.
30. Firas A Khasawneh, Elizabeth Munch, and Jose A Perea. Chatter classification in turning using machine learning and topological data analysis. *IFAC-PapersOnLine*, 51(14):195–200, 2018.
31. Grzegorz Muszynski, Karthik Kashinath, Vitaliy Kurlin, Michael Wehner, et al. Topological data analysis and machine learning for recognizing atmospheric river patterns in large climate datasets. *Geoscientific Model Development*, 12(2):613–628, 2019.
32. Jacob Townsend, Cassie Putman Micucci, John H Hymel, Vasileios Maroulas, and Konstantinos D Vogiatzis. Representation of molecular structures with persistent homology for machine learning applications in chemistry. *Nature communications*, 11(1):3230, 2020.
33. Zhenyu Meng and Kelin Xia. Persistent spectral-based machine learning (perspect ml) for protein-ligand binding affinity prediction. *Science advances*, 7(19):eabc5329, 2021.
34. Chi Seng Pun, Si Xian Lee, and Kelin Xia. Persistent-homology-based machine learning: a survey and a comparative study. *Artificial Intelligence Review*, 55(7):5169–5213, 2022.
35. E Bruce Goldstein. *Sensation and perception*. Wadsworth/Thomson Learning, 1989.
36. Greg Hamerly and Charles Elkan. Alternatives to the k-means algorithm that find better clusterings. In *Proceedings of the eleventh international conference on Information and knowledge management*, pages 600–607, 2002.
37. James R Munkres. *Elements of algebraic topology*. CRC press, 2018.
38. Clément Maria, Jean-Daniel Boissonnat, Marc Glisse, and Mariette Yvinec. The gudhi library: Simplicial complexes and persistent homology. In *Mathematical Software–ICMS 2014: 4th International Congress*, Seoul, South Korea, August 5-9, 2014. *Proceedings 4*, pages 167–174. Springer, 2014.

Acknowledgments

This work is supported by the National Natural Science Foundation of China under Grant Nos. 62272406 and 61932018.

Author contributions statement

Y.C. and H.L. carried out the theoretical analysis and wrote the manuscript. Y.C. and J.Y. devised the experiments. All authors participated in editing the manuscript.

Competing interests

The authors declare no competing interests.

Additional information

Supplementary Information is available for this paper.